

Transport in magnetically ordered Pt nanocontacts

J. Fernández-Rossier, D. Jacob, C. Untiedt, and J. J. Palacios

Departamento de Física Aplicada and Instituto Universitario de Materiales de Alicante (IUMA), Universidad de Alicante, San Vicente del Raspeig, 03690 Spain.

(Dated: April 11, 2018)

Pt nanocontacts, like those formed in mechanically controlled break junctions, are shown to develop spontaneous local magnetic order. Our density functional calculations predict that a robust local magnetic order exists in the atoms presenting low coordination, i. e., those forming the atom-sized neck. In contrast to previous work, we thus find that the electronic transport can be spin-polarized, although the net value of the conductance still agrees with available experimental information. Experimental implications of the formation of this new type of nanomagnet are discussed.

PACS numbers:

Fabrication of metallic nanocontacts permits to probe the electronic and mechanical properties of conventional metals with unconventional atomic coordination¹. Electron transport in these systems depends on the tiny fraction of atoms in the sample forming the atom-sized neck which have a reduced coordination and are responsible for the two-terminal resistance. Transport experiments can thereby probe the atomic and related electronic structure of these atoms and provide information about a fundamental question: How bulk properties evolve when the system reaches atomic sizes and atoms with full bulk coordination are no longer majority. A bulk property that is susceptible to change is magnetism. Bulk Pt, for instance, is a paramagnetic Fermi liquid with a rather large spin susceptibility². A transition to a ferromagnetic state could be expected upon reduction of the atomic coordination with the concomitant increase of the density of states at the Fermi energy beyond the Stoner limit. Density functional calculations^{3,4,5} for one-dimensional infinite Pt chains support this hypothetical scenario, resulting in a ferromagnetic transition above a critical lattice spacing which, depending on the computational approach, can be below the equilibrium lattice constant⁴. The formation of local moments in real Pt nanocontacts would not be totally unexpected.

Formation of and electronic transport in finite Pt chains, for instance, have been extensively studied experimentally^{8,9,10,11,12}. Based upon the appearance of a peak at $G = 0.5 \times 2e^2/h = 0.5G_0$ in the conductance histogram Rodrigues *et al.* suggested that Pt and Pd nanocontacts could be spin polarized¹². The origin of this peak has been later attributed to adsorbates¹³ so that magnetism in Pt and Pd nanocontacts has not been confirmed experimentally yet. Previous theory work has addressed the formation of local moments in Pd nanocontacts⁶ and in Co, Pd and Rh short chains sandwiched between Cu planes⁷. To the best of our knowledge theory work on Pt nanocontacts^{14,15,16,17,18} has overlooked the possibility of local magnetic order so far. Here we perform density functional calculations of both the electronic structure and transport and find that local magnetic order can develop spontaneously in Pt

nanocontacts. Local magnetic moments as high as $1.2 \mu_B$ in low-coordination atoms are found. Interestingly, while transport is definitely spin polarized, the calculated total conductance of magnetic and non-magnetic Pt nanocontacts is very similar and in agreement with experimental data, explaining why magnetism has been unnoticed so far.

The rest of the paper is organized as follows. First we discuss the methodology of the electronic structure calculation presented here. Second we present results for idealized infinite and finite one-dimensional Pt chains. Then we calculate both zero-bias transport and the electronic structure of Pt nanocontacts, which turn out to be magnetic beyond attainable values of the stretching. Finally we discuss whether magnetism in Pt nanocontacts is robust to thermal and quantum fluctuations, and propose experimental verification of the different scenarios. We also comment on the effect of spin-orbit interaction, missing in our calculations.

Electronic structure and transport calculations.— The electronic structure of various low dimensional structures of Pt which mimic actual nanocontacts are calculated in the density functional approximation, using either CRYSTAL03¹⁹ or ALACANT (Alicante Ab initio Computation Applied to Nanotransport), our *ab initio* transport package²⁰ interfaced to GAUSSIAN03²¹. ALACANT describes the bulk electrodes using a semiempirical tight-binding Hamiltonian on a Bethe lattice. The spin-resolved density matrix includes the effect of the electrodes by means of self-energies and the spin-polarized transport^{22,23} is obtained with the standard Landauer formula. Both GAUSSIAN03/ALACANT and CRYSTAL03 perform electronic structure calculations using a basis of localized atomic orbitals (LAO). CRYSTAL03 permits to calculate infinite systems with crystalline symmetry whereas ALACANT is suitable for systems with no symmetry or periodicity such as nanocontacts in or out-of-equilibrium situations. In the case of the Pt calculations shown here we use scalar relativistic (SR) pseudopotentials for the 60 inner electrons and the remaining 18 electrons are treated using generalized gradient approximation (GGA) density functionals. The

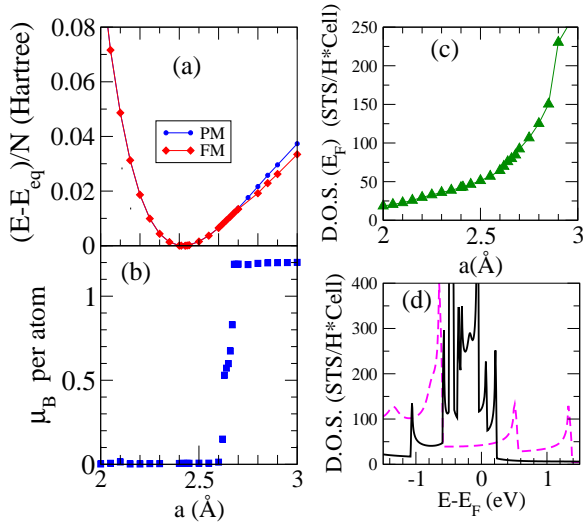


FIG. 1: (Color online). (a) Energy per atom for a perfect monostrand Pt chain. (b) Magnetic moment per atom as a function of lattice spacing a . (c) Density of states (D.O.S.) of the paramagnetic chain at the Fermi energy as a function of a . (d) D.O.S. as a function of energy for $a = 2.4\text{\AA}$ (dashed) and $a = 2.8\text{\AA}$ (solid)

basis set used for all the calculations has been optimized to describe bulk Pt as well as Pt surfaces²⁴. Other basis sets such as LANL2DZ or SDD²¹ have occasionally been employed for comparison. The main results do not depend on the choice of basis set.

Results.— We first consider a perfect one-dimensional mono-strand Pt chain. Such an idealized system serves as a standard starting point to understand lower symmetry geometries. It also permits to test whether our LAO pseudopotential methodology reproduces the results obtained with SR all electron plane-wave calculations reported by Delin *et al.*⁴. In Fig. 1(a) we show the energy per atom as a function of the lattice constant a both for the paramagnetic (PM) and the ferromagnetic (FM) chain. They both have a minimum at $a = 2.4\text{\AA}$. The FM chain develops a non-negligible magnetic moment when the lattice constant goes beyond $a \simeq 2.6\text{\AA}$. This configuration is clearly lower in energy above that distance. The energy difference between the FM and the PM configurations is 16 meV per atom for $a = 2.7\text{\AA}$ and 33 meV per atom for $a = 2.8\text{\AA}$. The magnetic moment per atom reaches a saturation value of $1.2\mu_B$. The equilibrium distance, critical spacing, asymptotic magnetic moment and shape of the phase boundary obtained by us are similar to those obtained by Delin *et al.*⁴ using a SR all-electron plane-wave calculation. Our results and those of Delin *et al.* underestimate the onset of the magnetic transition compared to calculations including spin-orbit coupling^{4,5} that predict that a magnetic moment forms already below the equilibrium distance.

The magnetic transition in the phase diagram [Fig. 1(b)] is compatible with the Stoner criterion for ferromagnetic instability. As the chain is stretched, the atom-

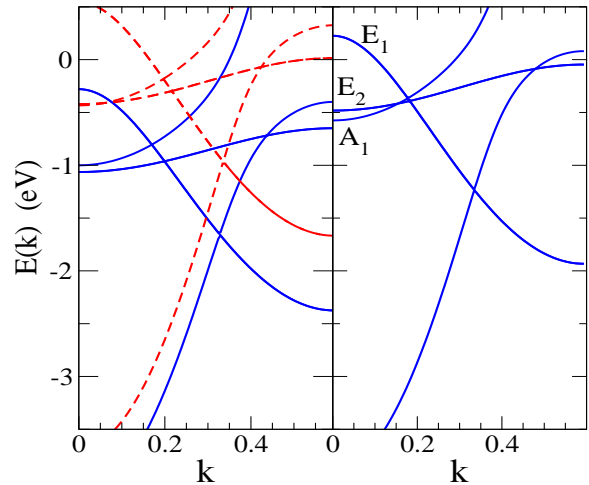


FIG. 2: (Color online). Energy bands for ideal Pt chain with $a = 2.8\text{\AA}$. Left: ferromagnetic phase. Right: paramagnetic case.

atom coupling becomes weaker, the bands narrow down and so does the density of states ($\rho(\epsilon)$). Since the integrated $\rho(\epsilon)$ must be equal to the number of electrons per atom, narrowing of the DOS implies an increase of the $\rho(\epsilon)$ [see Fig. 1(d)] and, therefore, an increase of the spin susceptibility, which is proportional to $\rho(\epsilon_F)$. In Fig. 1(c) we show how the $\rho(\epsilon_F)$ of the PM chain increases as a function of the lattice constant. The remarkable feature of Pt chains is that the Stoner instability occurs close to the equilibrium lattice spacing.

The electronic structure of the ideal Pt chain sheds some light on the electronic structure of the nanocontact. In Fig. 2 we show the energy bands for the ideal Pt chain both in the FM (left panel) and PM (right panel) configurations, for a lattice spacing $a = 2.8\text{\AA}$. We notice that the spectrum at $k = 0$ has four resolved energy levels per spin. These correspond to the $6s$ level, and the $5d$ levels which, because of the axial potential created by the neighboring atoms, split into 2 doublets E_1 , E_2 and one singlet A_1 . The E_1 and E_2 are linear combinations of orbitals with $L_z = \pm 1$ and $L_z = \pm 2$, respectively, whereas the A_1 singlet is a $L_z = 0$ orbital that hybridizes with the lower energy $6s$ orbital. The largest contribution to the density of states, and therefore to the magnetic instability, comes from the A_1 -like band at the edge of the Brillouin zone. However, the prominent role played by these bands in the magnetic behavior of Pt chains is in stark contrast with their role on the transport properties of Pt nanocontacts (see below and see also related work on Ni nanocontacts²³). Four spin-degenerate bands cross the Fermi energy in the PM case whereas 7 spin-split bands do it in the FM chain. In the FM chains the number of spin minority channels is 6, and the number of spin majority channels is 1. Although spin-orbit interaction modifies significantly the bands⁴, the number of bands at the Fermi energy is pretty similar in both cases. Therefore, one can anticipate that the number

of open channels in the magnetic and non-magnetic Pt nanocontacts studied below should be roughly the same and thereby the conductance should be similar, although the spin polarization might well be large in the former case. The conductance of the ideal FM chain is $3.5G_0$, very far from the value of $0.5G_0$ that allegedly signals the emergence of magnetism and also far away from half of the conductance of the PM chain, so it is very unlikely that the celebrated half quantum can be attributed exclusively to magnetism.

Real Pt chains are typically less than five atoms long and are connected to bulk electrodes. Although not surprising, we have verified that magnetism survives in isolated short chains with $N_A = 3, 4$ and 5 Pt atoms. The equilibrium distance is 2.4\AA for all $N_A = 3$, $N_A = 4$, and $N_A = 5$. Interestingly, the short chains are always magnetic in the $N_A = 3$ and $N_A = 4$ cases and show a non-magnetic to magnetic crossover at $a = 2.6\text{\AA}$ in the $N_A = 5$ case, already similar to the ideal infinite chain. The total magnetic moment of all the $N_A = 3$ chains with $a < 3.0\text{\AA}$ is $4\mu_B$. The outer atoms have a magnetic moment of $1.36\mu_B$ and the central atom with larger coordination has a smaller magnetic moment of $1.29\mu_B$. In the case of $N_A = 4$ the total magnetic moment is $6\mu_B$, and their distribution is similar to the $N_A = 3$ case.

The calculations above show that magnetism is present both in finite- and infinite-sized Pt systems with small atomic coordination. It remains to be seen that this holds true in nanocontacts where none or only few atoms have a small coordination (like in the case of formation of short chains), but these are strongly coupled to the bulk. In order to verify whether or not this is the case, we have calculated both electronic structure and transport for a model Pt nanocontact. It is formed by two opposite pyramids grown in the (001) crystallographic orientation of bulk Pt and joined by one atom which presents the lowest possible coordination [see inset in Fig. 3(a)]. Relaxation of the 11 inner atoms of the cluster has been performed starting from an equilibrium situation as a function of the distance d of the outer planes. Zig-zag configurations appear in the chain for small values of d (not shown)¹⁸ until the three-atom chain straightens up (see inset in Fig. 3(a)] followed by a plastic deformation (not shown). This deformation can be in the form of a rupture or a precursor of the addition of a new atom to the chain which comes from one of the two 4-atom bases³.

We now compute the transmission before the plastic deformation occurs (left panel in Fig. 3), where the atom-atom distance in the short chain is 2.82\AA . The value of the corresponding atomic-plane-averaged magnetic moments are also shown in the inset. As expected, it decreases for atoms in the bulk as the coordination reaches the bulk value. Some atomic realizations in the stretching process (like zig-zag ones) result in nanocontacts with smaller Pt-Pt distance and no magnetism, in agreement with the infinite chain phase diagram in Fig. 1. In contrast to the infinite chain, there are only three channels contributing to the total conductance for mi-

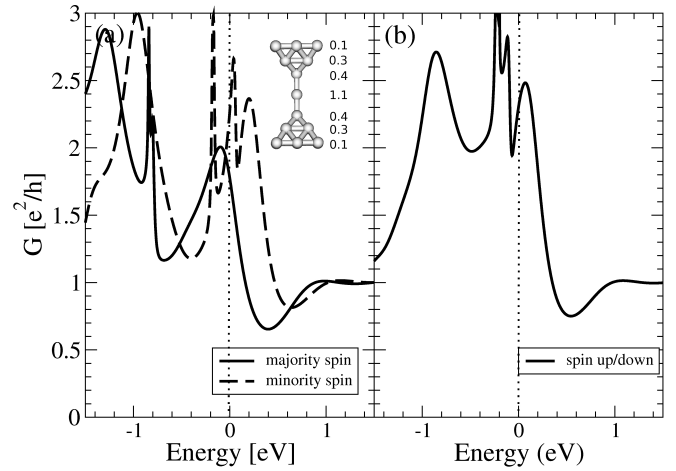


FIG. 3: Conductance per spin channel for a nanocontact with a 3-atom Pt chain (see inset) for the magnetic solution (a) and the non-magnetic one (b). The atom-atom distance in the chain is 2.8\AA .

nority electrons and there are more than one (three) for majority ones. For the majority electrons these are a perfectly transmitting s -type channel and two partially open ($T = 0.4$) pd -type channels (one $p_x d_{xz}$ - and one $p_y d_{yz}$ - hybridized). The three minority channels have the same character as the majority channels, except that here the s -type channel does not transmit perfectly while the transmission of two pd -type channels is enhanced so that all three minority channels have a transmission around 0.7. The other two remaining pd -like channels are responsible for the sharp resonances that appear around the Fermi level. The total conductance of the nanocontact in the FM case thus turns out to be around $4e^2/h = 2G_0$ which is only slightly larger than the average experimental value corresponding to the last plateau ($1.75G_0$), but, interestingly, barely differs from the value obtained when the possibility of magnetic order is ignored [around $2.3G_0$, see right panel in Fig. 3]. As in the case of the ideal chain, the FM conductance is not half of the PM conductance nor half of G_0 . To conclude this discussion we notice the, although transport is only weakly spin polarized, magnetism brings the pd -like resonances up to the Fermi level compared to the non-magnetic case. These resonances may well give features in the low bias conductance not present if Pt were not magnetic.

Conclusions and Discussion.— The main conclusion of this work is that density functional calculations predict that nanochains formed in Pt nanocontacts can be stretched as to become magnetic. The magnetic moment is localized mainly in the atoms with small coordination and does not modify appreciably the total conductance, although the transmission is moderately spin polarized. How robust are these results? It is well known that both local and gradient-corrected density functionals present some degree of electronic self-interaction, in contrast with the Hartree-Fock approximation. Self-interaction

is larger for localized electrons and shifts the the d bands upwards in energy, as shown in the case of Co, Ni and Pd one dimensional chains²⁵. A number of schemes to avoid this problem, like LDA+U and Self-Interaction Correction functionals have been proposed. The method of choice between chemist is hybrid functionals²⁶ in which local and Hartree-Fock exchanged are combined and the self-interaction is reduced. We have calculated the magnetic phase diagram of the one dimensional Pt chain using the hybrid B3LYP functional²⁶ and found, somewhat expectedly, that magnetism is enhanced and that B3LYP infinite Pt chains are ferromagnetic down to the equilibrium distance ($a = 2.4$ Å). Both non-local exchange and spin-orbit coupling⁴ enhance the stability of magnetism in Pt nanocontacts. This and previous results on Ni nanocontacts²³ lead us to believe that self-interaction is an issue in the electronic structure and transport properties of transition metal nanocontacts and further work is necessary along these lines²⁷.

The mean field picture of the electronic structure describes a static magnetic moment without preferred spatial direction. In reality the nanomagnet formed in the break junction is exchanged coupled dynamically to the Fermi sea of the conduction electrons of the electrodes. In the case of a spin $S = 1/2$ this can result in the formation of a Kondo singlet that would yield an anomaly in the zero bias conductance. For larger spins, the conduction electron sea cannot screen the spin completely so that the magnetic moment survives. The magnetic moment of the nanocontact in Fig. 3 is $S \approx 6$, compa-

table to that of single molecule magnets²⁸, making the formation of a Kondo singlet unlikely.

In the absence of spin-orbit interactions and external magnetic field a electronic configuration with total spin S has $2S + 1$ degenerate configurations corresponding to the spin pointing along different directions. However, spin-orbit interaction is strong in Pt and produces spin anisotropy, favoring orientation along the transport direction axis in the case of one dimensional chains⁴. Thermal fluctuations of the magnetic moment between these two configurations are quenched for temperatures smaller than the anisotropy barrier. Departures from the easy axis orientation will be damped via electron-hole pair creation across the Fermi energy that would also result in small bias features in transport³¹. The application of a sufficiently strong magnetic field in the direction perpendicular to the easy axis moves the local magnetic moments away from their easy axis. This is known to change the number of open channels at the Fermi energy in both the case of Ni ideal chains²⁹ and in the case of ferromagnetic semiconductor tunnel junctions³⁰. This effect, or maybe even larger, can be expected in Pt nanocontacts and could be used to detect the nanomagnetism experimentally.

Fruitful discussions with J. Ferrer are acknowledged. Work funded from Grants No. MAT2002-04429, FIS2004-02356, the Ramon y Cajal Program (MCyT, Spain), and Grant No. GV05/152 from Generalidad Valencina, are acknowledged. This work has been also partly funded by FEDER funds.

¹ N. Agrait, A. Levy-Yeyati, Jan M. van Ruitenbeek Physics Reports, **377** (2003) 81-279.

² A. H. MacDonald, J. M. Daams, S. H. Vosko, D.D. Koelling, Phys. Rev. B, **23** 6377 (1981)

³ S. R. Bahn and K. W. Jacobsen, Phys. Rev. Lett. **87**, 266101 (2001)

⁴ A. Delin, E. Tosatti, Phys. Rev. B, **68** 144434 (2003); A. Delin, E. Tosatti, Surf. Sci. **566-568**, 262 (2004).

⁵ T. Nautiyal, T. H. Rho, and K. S. Kim Phys. Rev. B, **69**, 193404 (2004).

⁶ A. Delin, E. Tosatti, R. Weht, Phys. Rev. Lett. **92**, 057201 (2004).

⁷ V. S. Stepnyuk, A. L. Klavsyuk, W. Hergert, A. M. Saletsky, P. Bruno, I. Mertig, Phys. Rev. B, **70**, 195420 (2004).

⁸ C. Sirvent *et al.*, Phys. Rev. B, **53**, 16086 (1996)

⁹ R. H.M. Smit *et al.*, Phys. Rev. Lett. **87**, 266102 (2001).

¹⁰ R. H.M. Smit *et al.*, Phys. Rev. Lett. **91**, 076805 (2003).

¹¹ S. K. Nielsen *et al.*, Phys. Rev. B, **67**, 245411 (2003).

¹² V. Rodrigues, J. Bettini, P. C. Silva and D. Ugarte, Phys. Rev. Lett. **91**, 096801 (2003).

¹³ C. Untiedt *et al.*, Phys. Rev. B **69**, 081401 (R) (2004).

¹⁴ L. de la Vega, A. Martín-Rodero, A. L. Yeyati, and A. Sal Phys. Rev. B 70, 113107 (2004).

¹⁵ Y. García *et al.*, Phys. Rev. B **69**, 041402R (2004).

¹⁶ V. M. García-Suárez *et al.*, Phys. Rev. B **72**, 045437 (2005).

¹⁷ K. S. Thygesen *et al.*, Phys. Rev. B **72**, 033401 (2005).

¹⁸ V. M. Garcia-Suarez *et al.*, cond-mat/0505487.

¹⁹ Crystal03 V. R. Saunders, R. Dovesi, C. Roetti, M. Caus N. M. Harrison, R. Orlando, and C. M. Zicovich-Wilson, CRYSTAL98 User's Manual, University di Torino, Torino 1998. CRYSTAL98 (manual).

²⁰ J. J. Palacios *et al.*, Phys. Rev. B **64** 115411 (2001); J. J. Palacios *et al.* Phys. Rev. B **66**, 035322 (2002); J. J. Palacios *et al.*, in *Computational Chemistry: Reviews of Current Trends*, ed. by Jerzy Leszczynski (World Scientific, Singapore, 2005).

²¹ M. J. Frish *et al.*, GAUSSIAN03, Revision B.01, Gaussian, Inc., Pittsburgh PA, 2003.

²² J. J. Palacios, Phys. Rev. B **72**, 125424 (2005).

²³ D. Jacob, J. Fernández-Rossier, J. J. Palacios, Phys. Rev. B **71**, 220403 (R) (2005).

²⁴ K. Doll, Surface Science **573**, 464 (2004).

²⁵ M. Wierzbowska, A. Delin, and E. Tosatti Phys. Rev. B **72**, 035439 (2005).

²⁶ A. D. Becke, J. Chem. Phys. 98, 5648 (1993).

²⁷ A. Ferretti *et al.*, Phys. Rev. Lett. **94**, 116802 (2005)

²⁸ A. Caneschi *et al.* J. Am. Chem. Soc. **113**, 5873 (1991)

²⁹ J. Velev *et al.*, Phys. Rev. Lett. **94**, 127203 (2005)

³⁰ L. Brey, C. Tejedor, J. Fernández-Rossier, Appl. Phys. Lett. **85**, 1996 (2004)

³¹ C. Untiedt and J. M. van Ruitenbeek, unpublished.